Single- and double-slit scattering of wavepackets

2002 J. Phys. A: Math. Gen. 35 4599

(http://iopscience.iop.org/0305-4470/35/21/309)

INSTITUTE OF PHYSICS PUBLISHING JOURNAL OF PHYSICS A: MATHEMATICAL AND GENERAL

J. Phys. A: Math. Gen. **35** (2002) 4599–4616 PII: S0305-4470(02)30667-X

Single- and double-slit scattering of wavepackets

G Kälbermann

Soil and Water Department, Faculty of Agriculture, Rehovot 76100, Israel

E-mail: hope@vms.huji.ac.il

Received 7 November 2001, in final form 26 March 2002
Published 17 May 2002
Online at stacks.iop.org/JPhysA/35/4599

Abstract

The quantum scattering of wavepackets from a single slit and a double slit with the Schrödinger equation is studied numerically and analytically. The phenomenon of diffraction of wavepackets in space and time in the backward region previously found for barriers and wells is encountered here also. A new phenomenon of forward diffraction that occurs only for packets thinner than the slit, or slits, is calculated numerically as well as in a theoretical approximation to the problem.

PACS numbers: 03.65.Nk, 42.25.Fx, 61.14.−x, 87.64.Bx

1. Introduction

In [1–4], the phenomenon of wavepacket diffraction in space and time was described both numerically in one and two dimensions [1, 2], as well as analytically in one and three dimensions [3]. The phenomenon occurs in wavepacket potential scattering for the nonrelativistic Schrödinger equation and for the relativistic Dirac equation.

The main feature of the effect consists in the production of a multiple-peak structure that travels in space. This pattern was interpreted in terms of the interference between the incoming spreading wavepacket and the scattered wave. The patterns are produced by a time-independent potential in the backward direction, in one dimension, and, at large angles, in three dimensions.

The multiple-peak wave train exists for all packets, but it does not decay only for packets that are initially thinner than $\sqrt{\frac{w}{q}}$, where w is a typical potential range or well width and q is the incoming average packet momentum. For packets that do not obey this condition, the peak structure eventually merges into a single peak.

This effect was named *wavepacket diffraction in space and time*. (See [3] for details.)

The present work addresses the paradigm of wave phenomena: diffraction from a single slit and a double slit, this time with wavepackets. The outcome of this study is twofold. In the backward region, the phenomenon of wavepacket diffraction will emerge, while in the forward region a new diffraction phenomenon will be found.

Diffraction phenomena from slits with electromagnetic waves [5], as well as matter wave diffraction from slits [6, 8], are treated by means of plane monochromatic waves. The Kirchhoff approximation [7], together with Green's theorem and Dirichlet boundary conditions, suffice to reproduce the alternating intensity structure on a screen or detector, the well-known Fresnel and Fraunhofer patterns in the forward region. In either case, the treatment of wavepackets is absent from the literature.

A smooth packet may be seen as made of a continuous spectrum of frequencies. From Huygens' principle it is expected that destructive interference between the various monochromatic components will generate a peak only in the forward direction. The thinner the incoming packet, the broader the energy–momentum spectrum. Therefore a very thin packet should by no means display a diffraction pattern. It is perhaps for this, and technological reasons, that there have not been any experimental searches and theoretical efforts to deal with the diffraction of wavepackets. There exist studies of electron diffraction with an electron microscope and of cold neutrons with crystals as reviewed in [8]. The experiments do not consider the packet structure.

The present work shows numerically and analytically that, contrary to the expectations, there appear diffraction patterns in the forward direction for packets that are thinner initially as compared to the slit dimensions.

Section 2 surveys briefly the phenomenon of diffraction of wavepackets in space and time that prompted this investigation. Numerical results for a single slit and a double slit are presented in this section. The results show that the wave in the backward region for narrow packets appears as a propagating multiple-peak wave train even in the region facing the slit holes. The theoretical analysis of this phenomenon follows directly from the formulae of [3]. Section 3 shows the results for the forward zone. The clear distinction between a thin packet and a wide, but finite, packet is evidenced by the existence or absence of a diffraction pattern.

A full analytical solution to the slit problem, even for plane waves, does not exist. There exists a treatment of wavepacket diffraction from slits with a separable ansatz [10]. However, this assumption is not valid, except perhaps at very large distances from the slit, or slits.

As an approximation to the exact analytical solution, the method of Green's functions is applied in section 3. The predicted patterns using the Kirchhoff approximation agree with the numerical results, except for thin packets.

Section 4 describes an improvement over the Kirchhoff approximation. The approach considers the added effect of the standing waves or cavity modes inside the slit. The ensuing diffraction pattern generated by the transient and cavity modes is called *cavity mode diffraction*. For extremely wide packets, resembling plane waves, the cavity modes contribution vanishes.

The long time behaviour of the forward scattering is depicted using the improved wavefunction. This aspect cannot be evaluated numerically at the present time, because it requires enormous computer time and memory. The theoretical predictions show that the pattern of a thin packet changes with space and time. It becomes extremely complicated as time evolves, but, it does not merge into a single peak as would have been expected. For extremely wide packets the predicted pattern is identical to that of a plane wave.

Section 5 summarizes the paper.

2. Slit diffraction in the backward region

Plane monochromatic waves in quantum mechanics show diffraction phenomena in time [11] induced by the sudden opening of a slit, or in space by fixed slits or gratings. The combined effect of time-dependent opening of slits for plane monochromatic waves produces diffraction

patterns in space and time [9]. These patterns tend to disappear as time progresses. Atomic wave diffraction experiments [12], have confirmed the predictions of Moshinsky [11] to be correct.

The phenomenon of diffraction of wavepackets in space and time was presented in [1–4]. It consists of a multiple-peak travelling structure generated by the scattering of initially thin packets from a time-independent potential, a well or a barrier.

In [3], analytical formulae for $t \to \infty$ were developed for the diffraction pattern of a scattering event of a wavepacket at a well or barrier.

In one dimension the amplitude of the wave in the backward region reads

$$\begin{aligned} |\psi(x,t)| &= 2\sqrt{\frac{2m\pi}{t}}\,\mathrm{e}^{-z}\left|\sin\left(\frac{mx}{t}\left(x_0+2\mathrm{i}\sigma^2 q_0\right)\right)\right| \\ &= 2\sqrt{\frac{2m\pi}{t}}\,\mathrm{e}^{-z}\sqrt{\sin^2\left(\frac{mxx_0}{t}\right)+\sinh^2\left(\frac{2\sigma^2 q_0 mx}{t}\right)} \qquad (1) \\ z &= \sigma^2\left(\frac{m^2\left(x^2+x_0^2\right)}{t^2}+q_0^2\right) \end{aligned}$$

where m is the mass, x_0 the location of the centre of the packet at $t = 0$, σ is approximately equal to the full width at half maximum of the packet for a Gaussian packet, and $q_0 = mv$, the average momentum of the packet.

This expression represents a diffraction pattern that travels in time. Equation (1) was compared to the numerical solution in [3], with excellent agreement and without resorting to any scale factor adjustment. (Figure 1 in [3].)

The condition for the pattern to persist, derived basically from equation (1), was found to be

$$\sigma \ll \sqrt{\frac{w}{q_0}}. \qquad (2)$$

The key element entering the derivation of the formula of equation (1), was the replacement of the real part of the reflection coefficient by its value at threshold, namely $\mathrm{Re}(R) = -1$. This replacement is valid for very long times at which the wild oscillations in the integrals that determine the reflected wave favour the contributions of very low momentum. The value at threshold is independent of the type of well or barrier. Hence the result holds in general. Depending on the initial width of the packet, a receding multiple-peak coherent wave train or a single hump will appear. This is the essence of the phenomenon of *wavepacket diffraction in space and time*. In three dimensions the travelling diffractive structure may occur at several angles [3].

The present work grew out of the interest in the case of slit diffraction in a laboratory for the phenomenon of wavepacket diffraction.

This section deals with the backward region for single- and double-slit scattering. The appearance of diffraction patterns in the forward region is discussed in section 4.

Figure 1 depicts the single slit set-up. Physical slits are usually infinitely long as compared to their width. Therefore a two-dimensional treatment is relevant. The impinging wave advances from the left towards the slit. The screen that defines the slit is taken as an impervious surface. In actual numerical calculations a large value for this repulsive potential, typically several orders of magnitude larger than the average kinetic energy of the packet, was used. Differing from the usual treatments of slit diffraction, the slit length $2a$ in figure 1 will play here a major role.

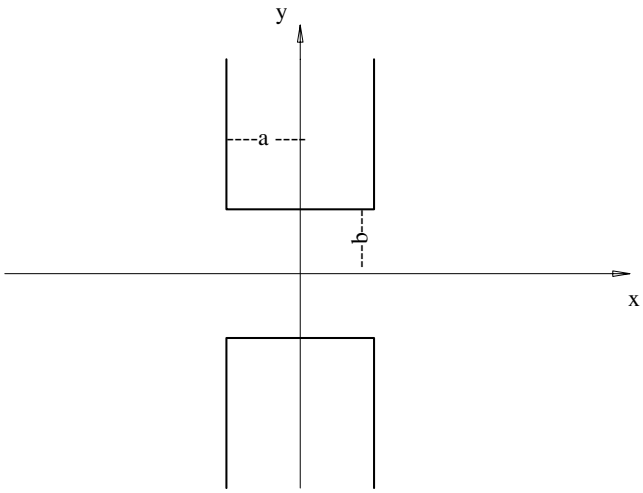

Figure 1. Slit geometry: $2a$ is the length of the slit and $2b$ the width.

The scattering event commences at $t = 0$ with a minimal uncertainty wavepacket

$$\Psi_0 = A\,\mathrm{e}^{w}$$
$$w = \mathrm{i}q_x(x - x_0) + \mathrm{i}q_y(y - y_0) - \frac{(x - x_0)^2}{4\sigma_1^2} - \frac{(y - y_0)^2}{4\sigma_2^2} \tag{3}$$

centred at a location x_0, y_0 large enough for the packet to be almost entirely outside the slit; σ_1, σ_2 denote the width parameters of the packet in the direction of the x, y axes, respectively, A is a normalization constant, and, $q_{x,y} = mv_{x,y}$ are the average momenta of the packet.

The algorithm for the numerical integration of the two-dimensional Schrödinger equation of the present work is a direct extension and refinement of the methods of [1–3][1]. The conservation of flux is verified by checking the normalization of the wave at the end of the process. Typically the flux is conserved to an accuracy better than 10^{-9} in all the runs.

Figure 2 depicts a 3D surface plot of the amplitude of the wave after $t = 300$ with parameters $x_0 = -10$, $y_0 = 0$, $v_x = 0.05$, $v_y = 0$, $\sigma_1 = 1$, $\sigma_2 = 1$ scattering off a slit with dimensions $a = 2$, $b = 3$ wider than the packet widths. The location of the slit is noted. The repulsive potential strength of the screen is $V_{\mathrm{screen}} = 10^{19}$, effectively infinite, but still amenable to numerical treatment.

The hilly structure in the backward region is the wavepacket diffraction in space and time studied in [1–4].

The diffractive structure exists even in a region facing the slit. This is in line with what was found before [3], concerning the appearance of wavepacket diffraction in space and time both for wells and barriers, as the opening may be considered to be a well inside a barrier.

In [1–4] it was found that for a wide packet the diffraction structure disappears. The same happens in the present case. Figure 3 shows the scattering event for the same input as in figure 1, except for the geometrical dimensions. The widths of the packet are now $\sigma_1 = \sigma_2 = 2$, while the dimensions of the slit are $a = b = 1$.

[1] The price paid is an extremely lengthy calculation time of almost a day of computer time in the VAXα cluster of the computation centre of the Hebrew University in Jerusalem for each and every run.

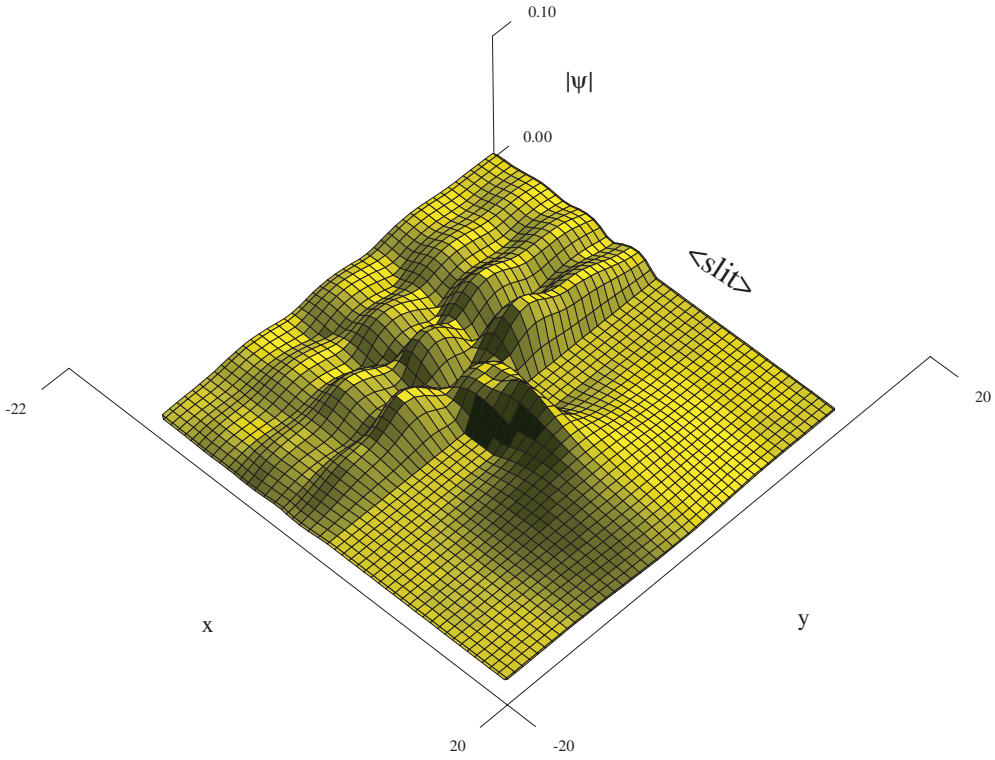

Figure 2. Single-slit 3D contour surface plot of the amplitude of the wave, for a thin packet, $\sigma_1 = 1, \sigma_2 = 1$, scattering off a slit with dimensions $a = 2, b = 3$.

The hilly structure disappears and, at the same time, the transmitted packet is negligible as compared to the thinner packet. Another feature that is evident from figures 2 and 3 is an interference pattern along the y axis.

The disappearance of the multiple peak structure is gradual and is influenced by the widths of the packet in the directions of both axes. The relevant parameter that determines the diffraction structure in the backward direction is the width of the packet in the horizontal direction. Even for relatively wide packets along the vertical axis the diffraction pattern still exists. This is evidenced in figure 4 where the same scattering event as in figure 1 is shown for different packet width parameters and slit dimensions.

Consider now a Young double slit arrangement as in figure 5.

Two scattering cases are depicted in figures 6 and 7. Figure 6 corresponds to the geometrical parameters for the slit $a = b = d = 2$, and the packet widths $\sigma_1 = \sigma_2 = 1$. Figure 7 corresponds to the geometrical parameters for the slit $a = b = 2, d = 2$ and the packet widths $\sigma_1 = 4, \sigma_2 = 5$.

The polychotomous peak structure appears here also for thin packets only.

In summary, the phenomenon of wavepacket diffraction in space and time applies to the single- and double-slit arrangements. The crucial parameter for its appearance is the thickness of the slit and screen. There exists also a diffraction pattern along the axis parallel to the screen. The origin of this pattern is evidently due to the interference between incoming and reflected waves as well as the waves excited inside the slit cavity. At this stage it was not possible to reproduce the qualitative features of this backward transverse pattern.

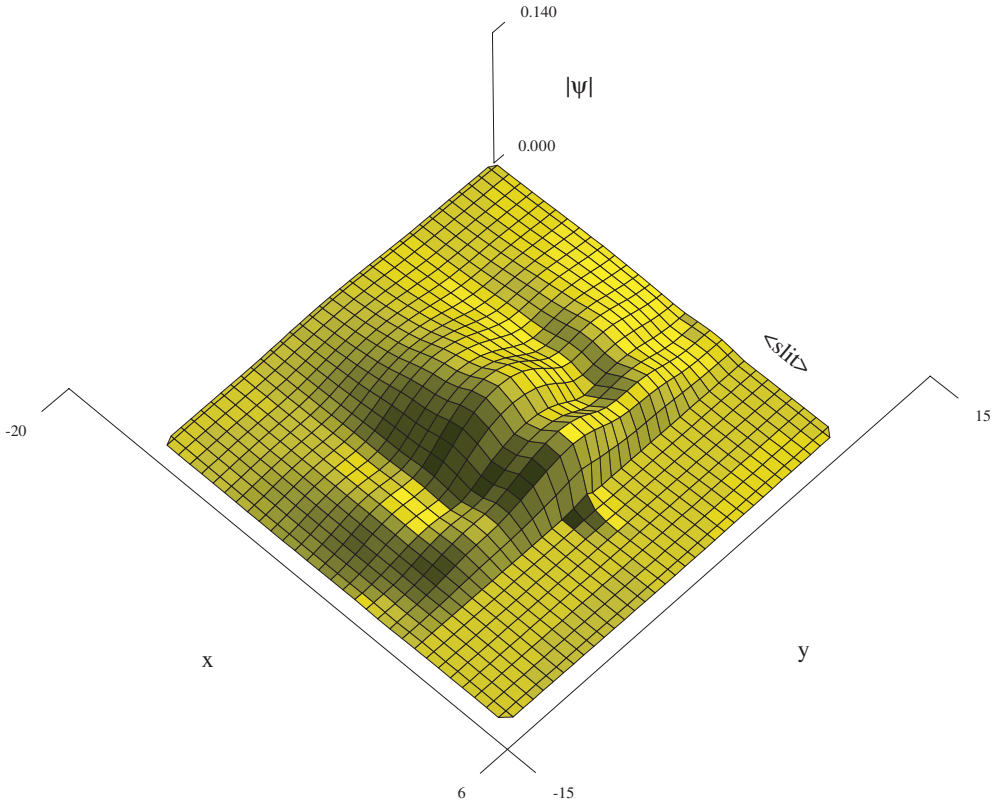

Figure 3. Single-slit 3D contour surface plot of the amplitude of the wave, for a wide packet. The widths of the packet are $\sigma_1 = \sigma_2 = 2$, while the dimensions of the slit are $a = b = 1$.

3. Single- and double-slit diffraction in the forward region

In the forward direction a very broad packet should behave effectively as a plane wave. A broad packet must then produce a diffraction pattern. On the other hand, very thin packets should not generate a diffraction structure. Only a broad central peak is to be present. The other maxima of the diffraction pattern have to disappear into the continuum because of destructive interference. These assertions find support in the Kirchhoff approximation to slit diffraction.

From Green's theorem, the Kirchhoff integral for the diffraction pattern from a slit with Dirichlet boundary conditions [9] may be readily written down. The wavefunction at a distance x, y from the centre of the slit located at the origin of coordinates reads [7, 8]

$$\Psi(\vec{r}, t) = \frac{1}{4\pi} \int_0^{t+} \mathrm{d}t_0 \int_{\text{opening}} \mathrm{d}\vec{S}_0 (G(\vec{r}, t, \vec{r}_0, t_0) \nabla_0 \Psi(\vec{r}_0, t_0) - \Psi(\vec{r}_0, t_0) \nabla_0 G(\vec{r}, t, \vec{r}_0, t_0)) \tag{4}$$

where G is the free propagator or Green's function for the Schrödinger equation

$$\begin{aligned} G(\vec{r}, t, \vec{r}_0, t_0) &= \Theta(\tau) \sqrt{\frac{m}{2\pi\, \mathrm{i}\tau^3}}\, \mathrm{e}^{\delta(\tau)} \\ \delta(t) &= \mathrm{i}m \frac{|\vec{r} - \vec{r}_0|^2}{2\tau} \end{aligned} \tag{5}$$

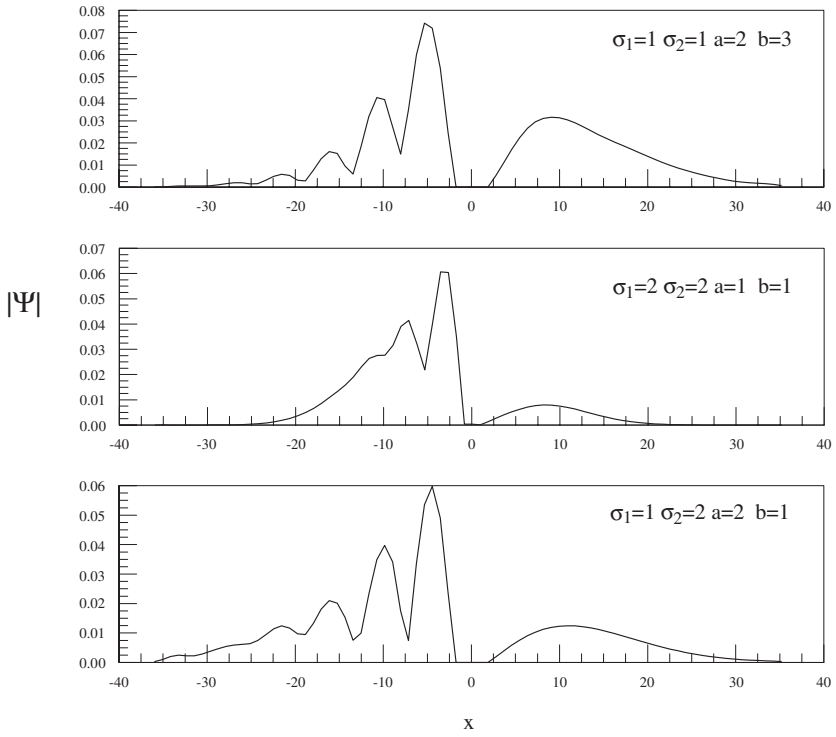

Figure 4. Wave amplitude as a function of x at a fixed $y = 5.46$ for various width and slit parameters.

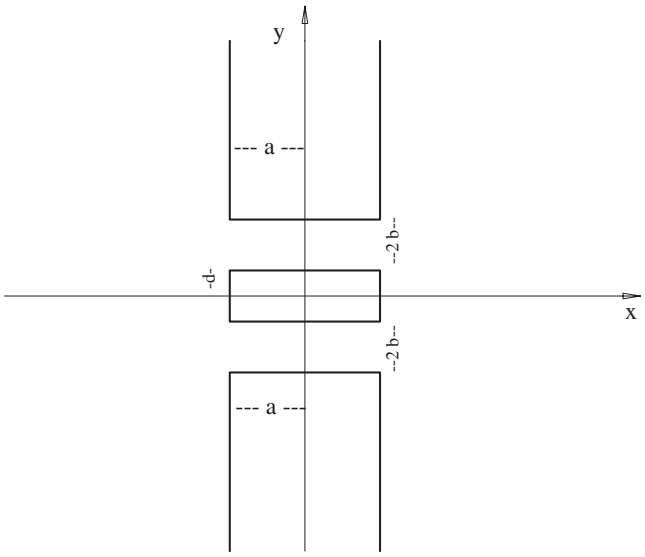

Figure 5. Geometry of the double-slit set-up.

where Θ is the Heaviside step function that guarantees causality, m is the mass of the particle and $\tau = t - t_0$, with $\hbar = 1$. The ∇ operator acts in the direction perpendicular to the opening,

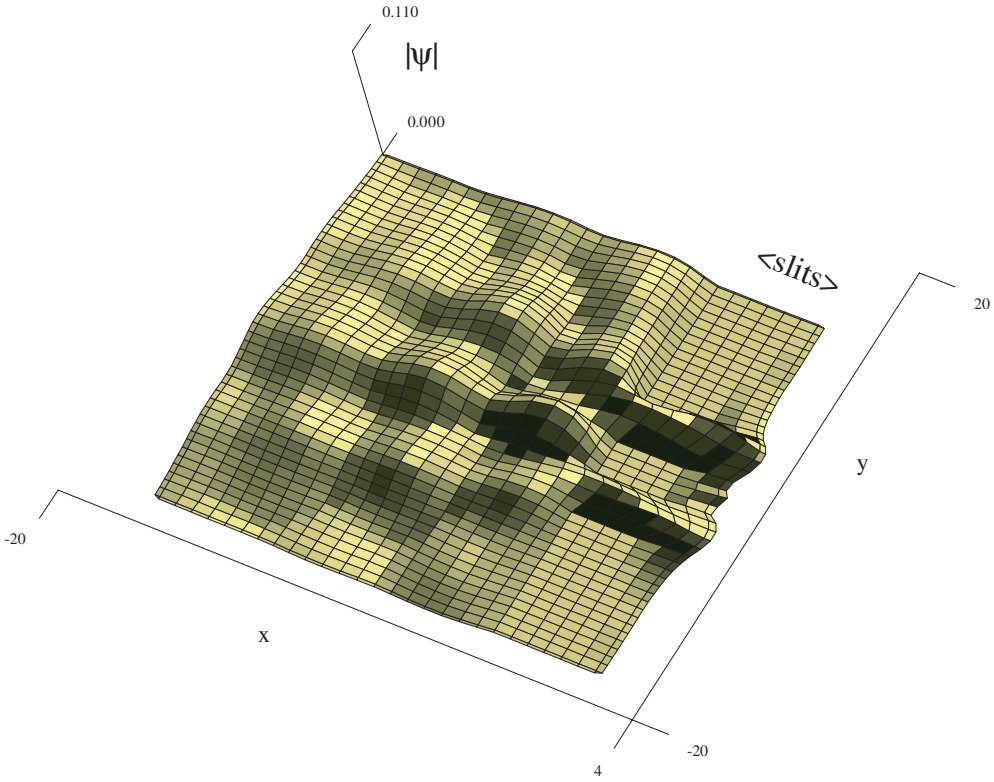

Figure 6. Double-slit 3D contour surface plot of the amplitude of the wave in the backward zone, for a thin packet. The geometrical parameters for the slit are $a = b = d = 2$, and the packet widths are $\sigma_1 = \sigma_2 = 1$.

the x-axis in the present case. The prediction of the diffraction pattern reduces now to the knowledge of the wave at the slit.

The next step that is usually taken at this stage is referred to as the *Kirchhoff approximation* [7]. The Kirchhoff approximation uses, for the wave at the slit, the same expression as that of the incoming wave behind the slit. This approach yields satisfactory results for plane waves and captures the main features of the diffraction patterns. In some cases it fails, and a full solution of the problem is needed. The Green's function approach becomes then of a limited value, similar to the limitations of the Born approximation in potential scattering. For the Schrödinger equation the results for plane wave diffraction from slits using the Kirchhoff approximation [8, 9], appear to be quite reasonable. It is then appropriate to take advantage of the above equation (4) for the case of wavepackets also.

The evaluation of the integrals of equation (4) is performed by resorting to the stratagem of rotating the time axis t_0. An alternative would be to integrate it using Fresnel integrals in the far field region. However, the interest of the present work is to compare to numerical results at all times and positions.

The rotation of the time axis should avoid crossing of poles or even passing through the vicinity of poles if no additional compensating terms are desired. The direction of the rotation has to be such that the integral still converges. This technique permits us to extend the integration over t_0 up to exactly $t_0 = t$. The method was tested against known diffraction expressions and found to be very accurate. Typically a rotation by an angle of

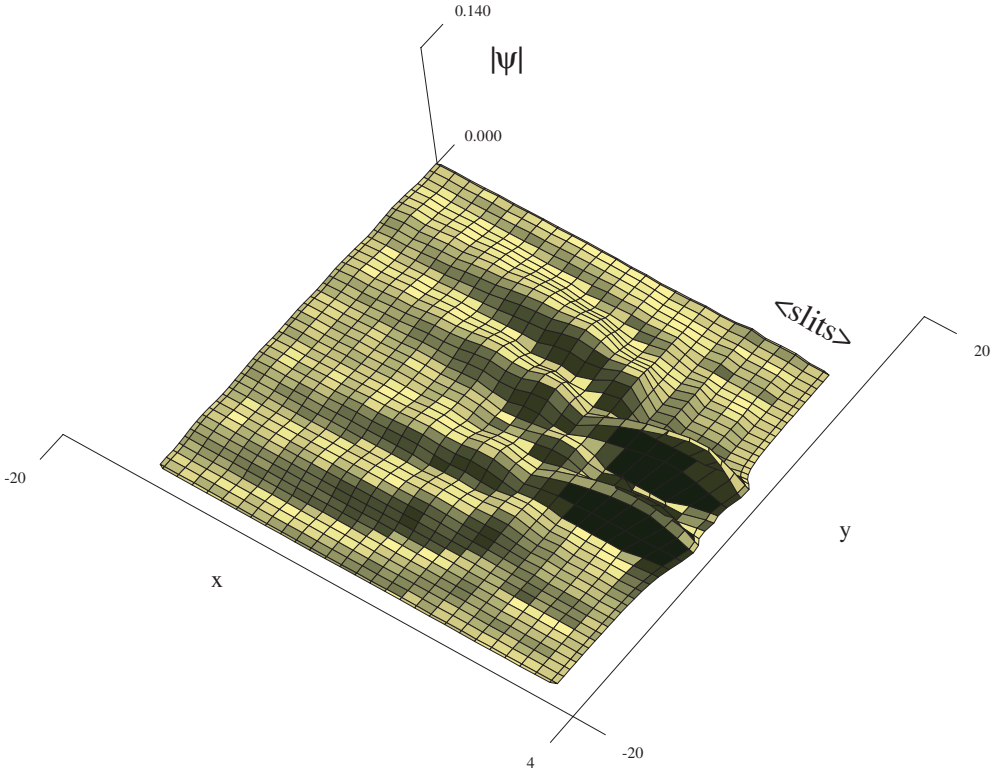

Figure 7. Double-slit 3D contour surface plot of the amplitude of the wave in the backward zone, for a wide packet. The geometrical parameters for the slit are $a = b = 2$, $d = 2$ and the packet widths are $\sigma_1 = 4$, $\sigma_2 = 5$.

$\phi(t_0) \approx 0.001$, with around 10 000 integration points along the t_0 axis using double precision complex variables, was used.

For the slit of figure 1 that extends to infinity in the z direction, and the packet of equation (3), at $t_0 \neq 0$, the wavefunction becomes

$$\Psi(\vec{r}, t) = \frac{-\mathrm{i}mx}{4\pi} \int_0^{t+} \mathrm{d}t_0 \int_{-b}^{b} \mathrm{d}y_0 \, \Psi(0, y_0, t_0) \frac{\mathrm{e}^{\delta(\tau)}}{\tau^2} \left(1 - \frac{\mathrm{i}\tau(x_{00} + vt_0)}{2mx\left({\sigma_1}^2 + \frac{\mathrm{i}t_0}{2m}\right)} \right)$$
$$\delta(\tau) = \mathrm{i}m \frac{(y - y_0)^2 + x^2}{2\tau} \tag{6}$$

with the incoming packet given by

$$\Psi(0, y_0, t_0) = \sqrt{\frac{\sigma_1 \sigma_2}{2\pi}} \frac{\mathrm{e}^{-u}}{d_1 d_2}$$
$$u = \frac{(x_{00} + v_x t_0)^2}{4{\sigma_1}^2 d_1} + \frac{(y_0 - y_{00} - v_y t_0)^2}{4{\sigma_2}^2 d_2}$$
$$d_1 = {\sigma_1}^2 + \frac{\mathrm{i}t_0}{2m} \tag{7}$$
$$d_2 = {\sigma_2}^2 + \frac{\mathrm{i}t_0}{2m}$$

where now x_{00}, y_{00} denote the initial centre of the packet.

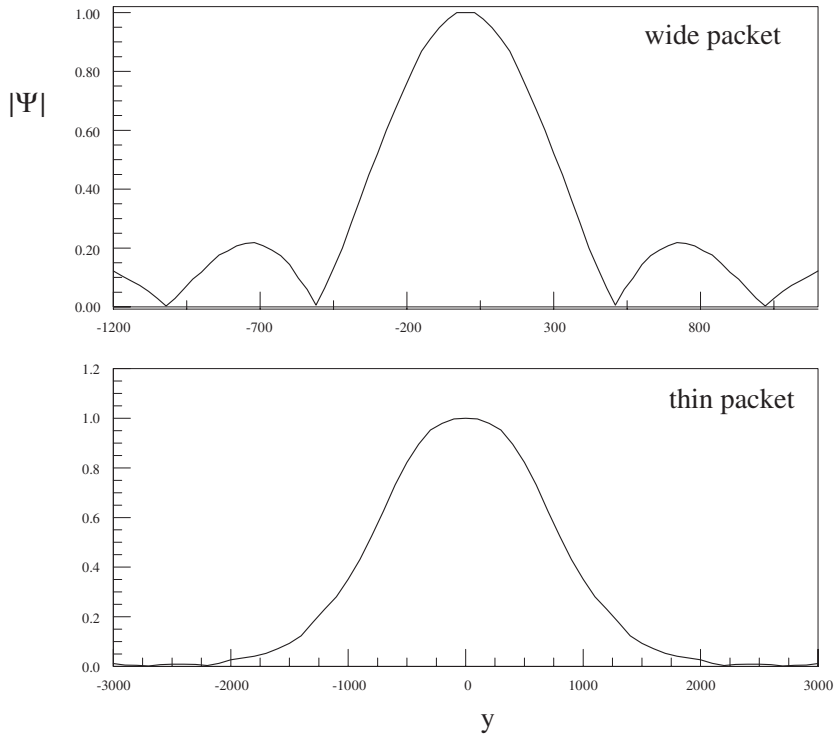

Figure 8. Amplitude of the wavefunction for the Kirchhoff approximation to the diffracted wave. The wide packet widths are $\sigma_1 = \sigma_2 = 100$, the thin packet widths are $\sigma_1 = \sigma_2 = 0.5$. The slit dimensions are $a = 2$, $b = 3$.

Figure 8 shows the long-time diffraction patterns for a wide packet and a thin packet in the Kirchhoff approximation of equation (6).

The wide packet $\sigma_1 = \sigma_2 = 100$, $x_0 = -200$, indeed has a diffractive structure, the thin packet $\sigma_1 = \sigma_2 = 0.5$, $x_0 = -10$, lacks it. The waves are normalized to one at $y = 0$ and the slit dimensions are $a = 2$, $b = 3$. The velocities are both taken to be $v = 0.5$, the mass is $m = 20$, and the time is $t = 10\,000$ at $x = 5000$ as a function of y.

The Kirchhoff approximation, considering only the slit opening and not its width, generates the expected diffraction pattern for a wide packet and a broad peak for a thin one.

However, the numerically calculated waves at finite times do not agree with the predictions of figure 8. Figure 9 depicts the numerical results for the amplitude of the wave for a thin packet at $x = 29.76$ as a function of y for the scattering event of a single slit, at $t = 300$ with initial parameters $x_0 = -10$, $y_0 = 0$, $v_x = 0.05$, $v_y = 0$, $\sigma_1 = 1$, $\sigma_2 = 1$ scattering off a slit with dimensions $a = 2$, $b = 3$ wider than the packet widths. The wave is renormalized to an amplitude equal to unity at $y = 0$.

For the thin packet a broad peak was expected but, instead, a structure resembling a diffraction pattern is obtained.

At the bottom of the figure the diffraction pattern disappears when the dimensions of the packet are large (but not infinite) as compared to the slit. This graph corresponds to a packet and slit with dimensions $\sigma_1 = 2$, $\sigma_2 = 1$, $a = 1$, $b = 2$.

The numerical results for various input parameters show that the crucial physical parameter for the appearance of a diffraction pattern is the ratio $\frac{\sigma_1}{a}$. For ratios larger than one no pattern

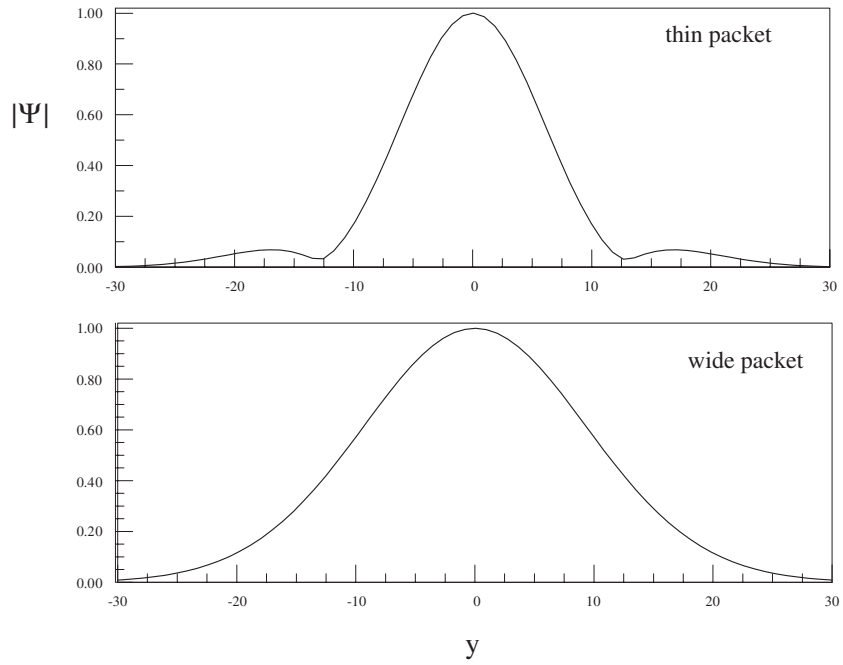

Figure 9. Numerical wave amplitude of the scattered wave at $x = 29.76$, as a function of y. The thin packet widths are $\sigma_1 = 1$, $\sigma_2 = 1$, for a slit with dimensions $a = 2$, $b = 3$. The broader packet picture corresponds to $\sigma_1 = 2$, $\sigma_2 = 1$, $a = 1$, $b = 2$.

was observed. This is analogous to the behaviour in the backward region for which a multiple-peak structure exists and persists only for packets that are initially thinner than the length of the slit.

The ratio $\frac{\sigma_2}{b}$ is also important, but the sensitivity is much less pronounced. It has to be quite large for the pattern to disappear. Figure 10 exemplifies this property. The upper curve is the same as the upper curve of figure 9, while the lower curve corresponds to a wide packet in the y direction, $\sigma_2 = 5$, $b = 1$. For $\sigma_2 < 5$, the diffraction pattern persists.

The forward diffraction along the vertical direction appears to be connected to the phenomenon of diffraction of wavepackets in space and time along the horizontal direction in the backward region.

The numerical results depicted in figures 9 and 10 suggest that the intuitive assumption of no diffraction for a thin packet is not borne out by the Schrödinger equation evolution of the packet. At the other end of plane waves, namely thin packets, somehow diffraction re-emerges.

In figure 11 the Kirchhoff approximation of equation (6) is calculated for both the thin and broad packets.

Although the shape is correct, the details of the diffraction structure for a thin packet are not reproduced by the Kirchhoff approximation. Many other numerical runs give the same results. The divide between thin and broad packets makes itself evident in the appearance, or lack of, a forward diffraction pattern. In the next section an improvement upon the Kirchhoff approximation is developed.

The results for the forward diffraction patterns in the double slit geometry of figure 5 are also very sensitive to the initial widths of the packets.

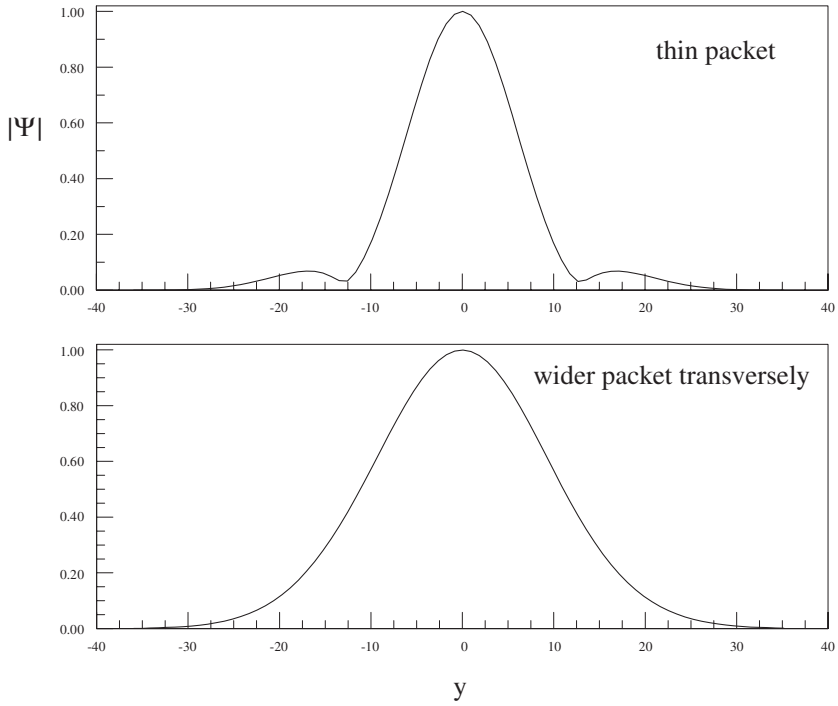

Figure 10. Numerical wave amplitude of the scattered wave at $x = 29.76$, as a function of y. The thin packet widths are $\sigma_1 = 1$, $\sigma_2 = 1$, and the wider packet widths are $\sigma_1 = 1$, $\sigma_2 = 5$. The slit dimensions are $a = 2$, $b = 3$, and $a = 2$, $b = 1$, respectively.

Figure 12 depicts the wave amplitude at $x = 35.16$ as a function of y, for an impinging packet with parameters $\sigma_1 = \sigma_2 = 1$, $x_0 = -10$, $y_0 = 0$, $v = 0.05$, $m = 20$, at $t = 300$, on the double slit of figure 5 with measures $a = b = d = 2$. The dotted line is the Kirchhoff approximation calculation of equation (6), with appropriately modified limits on the integration over y_0. The analytical results give qualitatively the broad features of the interference and diffraction patterns but as for the single slit case, they miss the details.

Figure 13 depicts the results for a wider packet on a smaller slit. The parameters are here $\sigma_1 = 4, \sigma_2 = 5$, $x_0 = -10$, $y_0 = 0$, $v = 0.05$, $m = 20$, at $t = 300$, $x = 15$ on the double slit of figure 5 with measures $a = b = 2$, $d = 1$. Reflections from the 'side walls' of the enclosure that define the integration region produce the spurious oscillations in the numerical results[2].

The dotted curve corresponds to the Kirchhoff approximation (6). Contrary to the thin packet case, the Kirchhoff approximation captures the main features of the pattern.

Figures 12 and 13 are consistent with the results for a single slit. The dimensions of the packets are relevant to the diffraction and interference structures seen. Thin packets generate diffraction and interference structures that are absent for wider packets. This effect is even more evident when the comparison to the Kirchhoff approximation is made. The Kirchhoff approximation works well for wide packets and misses the numerical results for thin packets. A very essential part of the scattered wave at the slit is not included in the Kirchhoff integral.

[2] Beyond $x = 15$, the oscillations increase and blur the picture. For a more reliable numerical calculation, a much larger area of integration is needed.

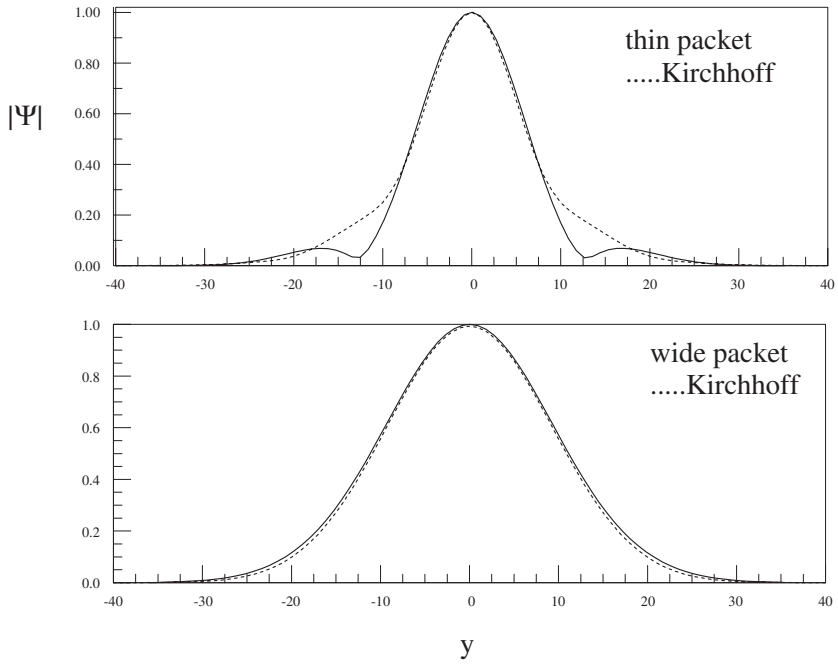

Figure 11. Comparison of the amplitude of the wavefunctions of figure 9 to the theoretical Kirchhoff approximation. The thin packet widths are $\sigma_1 = 1, \sigma_2 = 1$, for a slit with dimensions $a = 2, b = 3$. The broader packet picture corresponds to $\sigma_1 = 2, \sigma_2 = 1, a = 1, b = 2$.

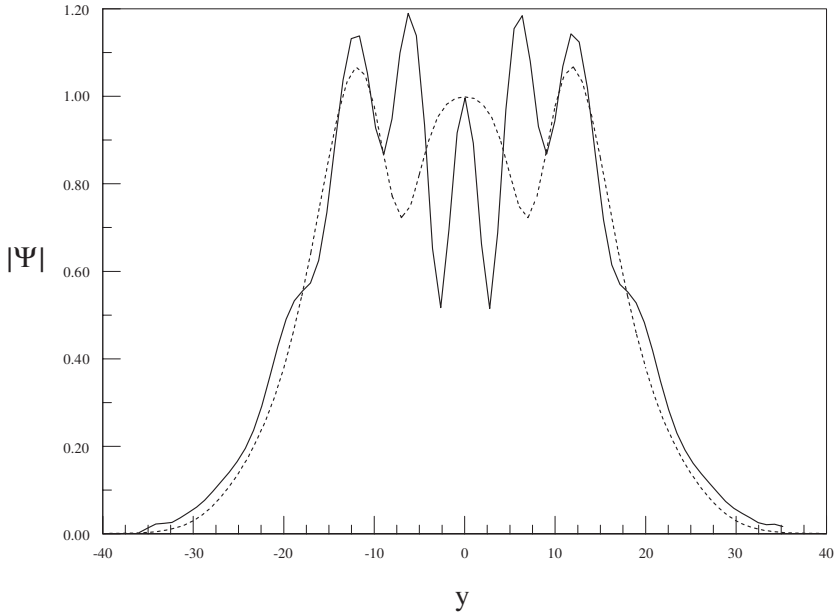

Figure 12. Double-slit interference pattern at $x = 35.16$ as a function of y for a thin packet, $\sigma_1 = \sigma_2 = 1$ (full line). Kirchhoff approximation of equation (6) (dotted line) for the double slit of figure 5 with measures $a = b = d = 2$.

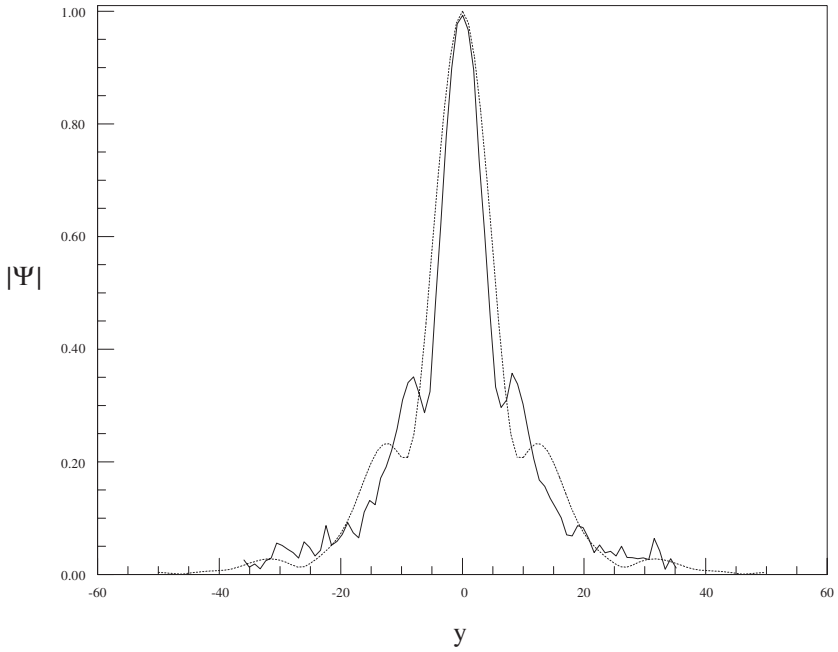

Figure 13. Double-slit interference pattern at $x = 15$ as a function of y for a wide packet of widths $\sigma_1 = 4$, $\sigma_2 = 5$ (full line), and Kirchhoff approximation of equation (6) (dotted line) for the double slit of figure 5 with measures $a = b = 2$, $d = 1$.

In section 4 it is proposed that this element may be the excitation of cavity modes inside the slit.

4. Cavity mode diffraction

The exact solutions to the single-slit problem are unknown, even for plane waves. It is intuitively apparent that the wavepacket inside the slit comprises transient waves and standing waves, as an electromagnetic wave in a Fabry–Perot interferometer [5]. The transient waves are already included in the Kirchhoff approximation. However, the cavity mode standing waves are not. The continuous spectrum of the incoming packet is decomposed inside the slit into a continuous background and a discrete spectrum. The reflected and transmitted waves take care of the continuity at the entrance and exit of the slit. The amplitude of the cavity modes has to decay with time. This behaviour was seen in the numerical solutions of [1, 2].

The cavity modes are already included in the spectrum of the incoming wave. However, they do not have there a prominent weight as compared to any other mode. Despite some amount of double counting that may be introduced by adding a specific contribution that singles out the cavity modes and, in the absence of an alternative way, the full wave at the slit will be taken to be the sum of the transient wave, the incoming packet with a continuum of modes and the standing waves with a discrete spectrum, the cavity modes. This procedure is somewhat analogous to the expansion of the wave at the slit in terms of the spectrum of a very deep well. This well may readily be disclosed by writing the cavity potential that is zero, as the large repulsive barrier of the screen, in addition to an attractive well of the same value.

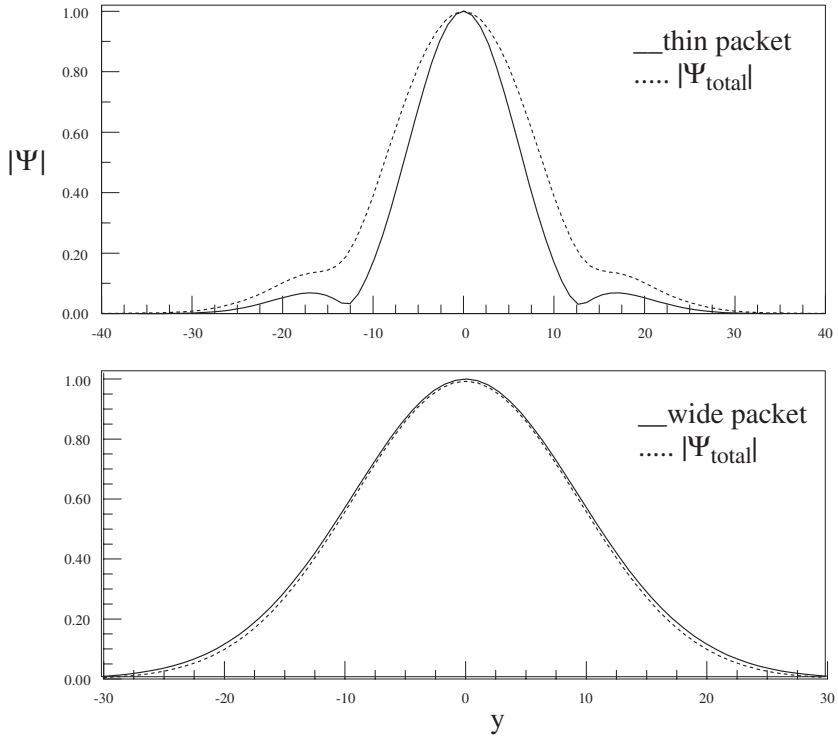

Figure 14. Comparison of the waves of figure 9 to the cavity mode plus incoming approximation, Ψ_{total}. The thin packet widths are $\sigma_1 = 1$, $\sigma_2 = 1$, for a slit with dimensions $a = 2$, $b = 3$. The broader packet picture corresponds to $\sigma_1 = 2$, $\sigma_2 = 1$, $a = 1$, $b = 2$.

The cavity modes with a Dirichlet boundary condition on the walls and the condition of having a standing wave with an antinode at the right end of the slit (without end correction) amount to the expansion

$$\begin{aligned} \Psi_{\text{cavity}} &= \sum_{p_n} A_n \cos(p_n(x-a)) \sum_{q_n} B_n \cos(q_n y) \\ p_n &= \frac{n\pi}{2a} \\ q_n &= \frac{(2n+1)\pi}{2b} \end{aligned} \tag{8}$$

where the origin has been shifted to the right-hand side of the slit. In order to find the coefficients, the *unknown* solution outside the slit-cavity is needed. At the left end of the cavity $x = -a$, the wave consists of the incoming wave, the reflected wave and the transmitted wave, both the continuum parts and the cavity modes. In a fully consistent treatment, both the function and the derivative have to be continuous. For the implementation of both continuity conditions, a respectable ansatz for the waves in all regions has to be assumed. In the absence of such an ansatz, the continuity of the function or the derivative—but not both—is able to determine, up to an overall scale, the B_n coefficients. The A_n coefficients are undetermined. The latter were fixed by comparing to the weight factors of the Fourier decomposition of the incoming wave[3].

[3] Other functional choices such as sine function, or exponential, or mixtures, gave inconsistent results for both a wide packet and a thin one.

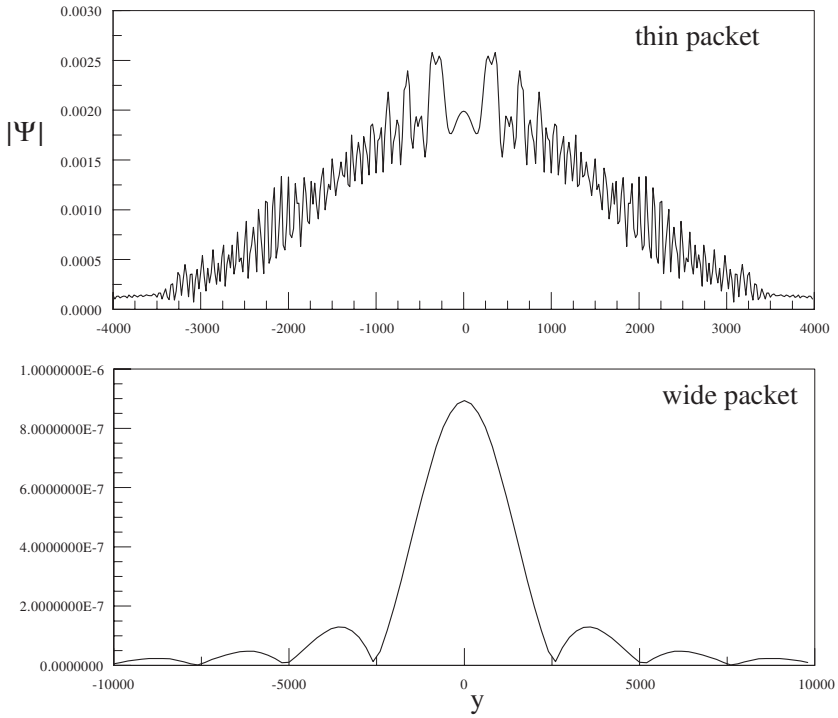

Figure 15. Calculated long time behaviour $t = 50\,000$, of the diffraction pattern of a thin packet as compared to a wide packet. The parameters are $\sigma_1 = \sigma_2 = 1$ for the single slit of figure 1 with measures $a = 2$, $b = 3$ for the upper graph, and $\sigma_1 = \sigma_2 = 100$, $x_0 = -200$ for the lower graph.

Up to an overall unknown phase (possibly time dependent) the amplitudes are then given by

$$A_n B_l = \sqrt{\frac{\sigma_1 \sigma_2}{2\pi}}\, \mathrm{e}^{-u} \cos(p_n(x_0 - a))$$
$$u = -\sigma_1^2 (p_n - mv)^2 - \sigma_2^2 q_l^2 - \mathrm{i}\frac{p_n^2 + q_l^2}{2m} t. \tag{9}$$

The total wavefunction is then $\Psi_{\text{total}} = \Psi_{\text{incoming}} + C\Psi_{\text{cavity}}$, where Ψ_{incoming} at the right-hand end of the slit is given in equation (6) and C is an unknown complex number. Comparing to the Fourier expansion of the incoming wave, the absolute value of this number should be of the order of $|C| \approx \frac{\pi^2}{4ab}$, the product of wavenumber increments.

Fortunately, the cavity modes and continuum contributions affect different regimes. The cavity mode piece is dominant for $\sigma_1 \approx \sigma_2 \approx 0$, the continuum contribution is negligible there (equations (3) and (9)). It is then not too worrisome that the exact value of C is not known. Ψ_{total} is now introduced in equation (4) in the slot of the wavefunction at the opening; the rest of the calculation proceeds as for the case of the Kirchhoff approximation explained above.

Figure 14 shows the numerical results together with Ψ_{total} for the single-slit diffraction pattern previously depicted in figures 9 and 11. It was shown there that the Kirchhoff approximation misses the diffraction pattern for a thin packet, whereas it reproduces the numerical calculation quite accurately for a wide one.

From figure 14 it is clear that the cavity modes play an important role in reproducing the thin packet results, while, at the same time, they do not spoil the fit to the wide packet case as expected.

The cavity modes are then an important ingredient in the diffraction pattern of thin packets, and are almost negligible for a wide packet.

After gaining some confidence with the approach, it is possible to look at the long time behaviour of the diffraction pattern, an aspect that cannot be obtained by numerical treatment at the present time. Although the results are presumably inaccurate quantitatively, the structure is expected to be relatively reliable. The calculation is presented in figure 15. The parameters are here $\sigma_1 = \sigma_2 = 1$, $x_0 = -10$, $y_0 = 0$, $v = 0.05$, $m = 20$, at $t = 50\,000$, $x = 5000$, on the single slit of figure 1 with measures $a = 2$, $b = 3$ for the upper graph, and $\sigma_1 = \sigma_2 = 100$, $x_0 = -200$ for the lower graph.

The wide packet pattern resembles the diffraction pattern of a plane wave, as expected. The thin packet produces a jagged structure with many peaks, some of them quite pronounced over the background.

5. Summary

In [1–4], the recently found effect of diffraction in space and time with wavepackets was addressed numerically and analytically. The diffraction pattern is evident in the backward zone in one dimension and at large angles in two and three dimensions. In the present work it was found that this backward effect appears also when packets scatter off slits.

The study of wavepacket scattering from slits has also uncovered a new diffraction effect. This effect emerges quite unexpectedly with thin packets in the forward direction. A thin packet may be viewed as a mixture of many frequencies; the thinner the packet, the wider the spectrum. Hence a single central peak is expected, and not any sidebands. The numerical results contradict this prejudice.

The effect of [1–4] was interpreted as a product of the interference between incoming and reflected waves. The forward diffraction pattern of the slits is here understood as resulting from the interference between incoming (transient) modes and the time-dependent excitation of standing waves inside the slit, thereby the name cavity mode diffraction.

The backward diffraction pattern appears as a hilly landscape along the propagation axis while the forward pattern appears across this direction.

The results of the present work suggest that there is a need for a revision and a renewed effort to solve this paradigm of matter waves scattering. On the experimental side, besides experiments with liquid helium, as simulated in [3], cold Bose gas packets may provide an appropriate setting for the investigation of the new diffraction phenomena on slits.

References

[1] Kälbermann G 1999 *Phys. Rev.* A **60** 2573
[2] Kälbermann G 2001 *J. Phys. A: Math. Gen.* **34** 3841 (*Preprint* quant-ph/9912042)
[3] Kälbermann G 2001 *J. Phys. A: Math. Gen.* **34** 6465 (*Preprint* quant-ph/0008077)
[4] Kälbermann G 2002 *J. Phys. A: Math. Gen.* **35** 1045 (*Preprint* cond-mat/0107522)
[5] Born M and Wolf E 1980 *Principles of Optics* (New York: Pergamon)
[6] Cowley J 1995 *Diffraction Physics* (Amsterdam: North-Holland)
[7] Jackson J D 1963 *Classical Electrodynamics* (New York: Wiley)

[8] Zeilinger A, Gähler R, Shull C G, Treimer W and Mampe W 1988 *Rev. Mod. Phys.* **60** 1067
[9] Brukner C and Zeilinger A 1997 *Phys. Rev.* A **56** 3804 and references therein
[10] Zecca A and Cavalleri G 1997 *Nuovo Cimento* **112** 1
Zecca A 1999 *Int. J. Theor. Phys.* **38** 1883
[11] Moshinsky M 1952 *Phys. Rev.* **88** 625
[12] Szriftgiser P, Guéry-Odelin D, Arndt M and Dalibard J 1997 *Phys. Rev. Lett.* **77** 4